Molecular Vision 2019; 25:283-294 <http://www.molvis.org/molvis/v25/283>
Received 10 April 2018 | Accepted 3 June 2019 | Published 5 June 2019

Altered expression of aquaporin 1 and aquaporin 5 in the cornea after primary blast exposure

José David Ríos,[1] Jae Hyek Choi,[2] Jennifer S. McDaniel,[1] Sandra Becera,[3] Leticia Bice,[1] Peter Johnson,[1] Jeffery M. Cleland,[1,9] Randolph D. Glickman,[4] Matthew A. Reilly,[5] Walt Gray,[6] William E. Sponsel,[7,8,9] Brian J. Lund[1]

[1]Department of Sensory Trauma, U.S. Army Institute of Surgical Research, San Antonio, TX; [2]Multi Organ Support Task Area, U.S. Army Institute of Surgical Research, JBSA Fort Sam Houston, San Antonio, TX; [3]Pathology Support Task Area, U.S. Army Institute of Surgical Research, JBSA Fort Sam Houston, San Antonio, TX; [4]Department of Ophthalmology, University of Texas Health Science Center, San Antonio, TX; [5]Department of Biomedical Engineering, Dept. of Ophthalmology, The Ohio State University, Columbus, OH; [6]Geological Sciences, University of Texas at San Antonio, San Antonio, TX; [7]Biomedical Engineering, University of Texas at San Antonio, San Antonio, TX; [8]WESMD Professional Associates, San Antonio, TX; [9]Rosenberg School of Optometry, University of the Incarnate Word, San Antonio, TX

Purpose: Our study aimed to determine whether the altered expression of biomarkers linked to corneal injuries, such as the edema-regulating proteins aquaporin-1 and aquaporin-5 (AQP1 and AQP5), occurred following primary blast exposure.

Methods: Adult male Dutch Belted rabbits were anesthetized and exposed to blast waves with peak overpressures of 142.5–164.1 kPa (20.4–23.4 psi). These exposure groups experienced peak blast overpressure-specific impulses (impulse per unit surface area) of 199.6–228.5 kPa-ms. Unexposed rabbits were included as controls. The animals were euthanized at 48 h post-exposure. Corneas obtained from the euthanized blast-exposed and control rabbits were processed for quantitative PCR and western blot to quantify mRNA and the protein expression of AQP1 and AQP5. Immunohistochemical analysis was conducted to determine the cellular localization of AQP1 and AQP5.

Results: Corneal thickness increased up to 18% with the peak blast overpressure-specific impulses of 199.6–228.5 kPa-ms at 48 h after blast exposure. mRNA levels of AQP1 and AQP5 increased in the whole cornea lysates of blast-exposed rabbits relative to those of the controls. Western blot analyses of whole cornea lysates revealed that the expression levels of AQP1 and AQP5 were approximately 2- and 1.5-fold higher, respectively, in blast-exposed rabbits compared to controls. The extent of AQP1 immunostaining (AQP1-IS) increased in the epithelial cell layer after blast exposure. The AQP5-IS pattern changed from a mixed membrane and cytoplasmic expression in the controls to predominantly cytoplasmic expression in the basally located cornea epithelial cells of blast-exposed rabbits.

Conclusions: Primary blast exposure resulted in edema-related changes in the cornea manifested by the altered expression of the edema-regulating proteins AQP1 and AQP5 with blast overpressure-specific impulses. These findings support potential acute corneal injury mechanisms in which the altered regulation of water permeability is caused by primary blast exposure.

Blast-related ocular injuries are of increasing concern in both military and civilian populations due to the potential long-term health problems and high treatment costs associated with recovery. Ocular injuries are the fourth most common battlefield injury sustained by military personnel, with an estimated incidence of 6%–13% among all blast injuries [1-3]. Ocular injury among blast victims is frequently linked to a combination of warfare tactics and the high-energy force of improvised explosive devices (IEDs) that are increasingly used by insurgents [1,2,4].

Generally, blast-induced damage of ocular structures results from a combination of different mechanisms. For example, a primary blast injury as the result of an explosive is caused by the blast wave itself, while changes in atmospheric pressure can create a shock wave impact to soft tissues. Specifically, the factors that influence the primary blast effect include the peak overpressure, its duration, the distance from the explosion, and the angle between the direction of the blast pressure wave and the eyes [5,6]. Other injury mechanisms include secondary blast injury from blast fragments, such as metal casing or flying debris from the explosive device.

Correspondence to: José David Ríos, Department of Sensory Trauma, U.S. Army Institute of Surgical Research, 3698 Chamber Pass, San Antonio, TX 78234, United States; Phone: (210) 539-8661; FAX: (210) 916-9687; email: jose.d.rios10.ctr@mail.mil

Tertiary blast injury occurs when displaced victims impact a stationary object with rapid deceleration. Severe chemical and/or thermal burns or other long-term effects (quaternary injuries) may also occur due to the explosive or other indirect injuries [5-7].

Despite clinical evidence regarding blast-induced ocular injury and many reports of visual dysfunction among blast victims, there is a paucity of studies on the pathological changes and molecular mechanisms associated with primary blast-induced ocular injury to the cornea [8]. It is noteworthy that recent studies involving rat and mouse models have found an increased expression of biomarkers associated with inflammation, oxidative stress, and apoptosis, as well as edema-regulating proteins (aquaporins or AQPs) in the retina, thus suggesting pathological changes associated with primary blast injuries [9-11]. It is also noteworthy that the increased levels of most of these biomarkers were observed immediately after blast exposure and were sustained up to two weeks, suggesting both acute and chronic phases of the injury [11].

In this context, our group previously showed that exposing rabbits to low-level blast overpressure generated by a large-scale shock tube resulted in corneal edema, evidenced by the increased thickness of corneal and retinal tissues associated with an acute manifestation of tissue swelling [12]. Corneal edema is the pathological condition of increased water content resulting from various coexisting corneal insults, including ocular surgery, trauma, infection, and secondary inflammation [13,14]. Consequently, the altered expression of AQPs is of great importance in the pathophysiology of corneal edema.

AQPs are transmembrane proteins that selectively allow the passage of water through the plasma membrane of fluid-transporting cells throughout the body [15]. To date, 13 subtypes of AQPs have been characterized, and AQP1, AQP3, and AQP5 have been found to be localized in the cornea [15,16]. AQP1 tends to be expressed in the plasma membrane of endothelial cells and stromal keratocytes in species as diverse as humans, mice, rats, cows, and rabbits [17-20]. Other subtypes, such as AQP3 and AQP5, are expressed in corneal epithelial cells in humans, mice, rats, and rabbits [17-19]. In rabbits, AQP3 is expressed in both the cornea and the conjunctiva [17].

Previous reports have demonstrated altered expression levels of AQP1, AQP3, and AQP4 in human corneas isolated from pseudophakic bullous keratopathy (PBK) and Fuchs' dystrophy (FD) patients, both of which exhibit corneal edema [21,22]. Here, we investigated the expression levels of AQP1 and AQP5 in the corneas of rabbits that were subjected to primary blast exposure, as previously studied by Jones et al. [12]. The focus of our study of these two AQPs stems from previous reports showing the high prevalence of AQP1 in rabbit corneas [17] and the implications of AQP1 and AQP5 in corneal epithelial wound healing [23,24]. Of the 13 subtypes of AQPs, AQP5 and AQP1 are major components of an osmotically driven water pathway across the corneal epithelium and endothelium, respectively [25,26]. Based on this, it is prudent to investigate the impact of blast injury on AQP1 and AQP5, as these proteins are well expressed in the cornea and may play an important role in edema related to blast injury.

We hypothesized that primary blast exposure would not only increase corneal thickness (CT) but also elevate the expression of biomarkers linked to corneal edema. Therefore, we evaluated the status of water channel AQPs (AQP1 and AQP5) in the cornea after primary blast wave exposure in a rabbit ocular blast injury model.

METHODS

Animals: This study used adult male Dutch Belted rabbits weighing 1.5–2.5 kg purchased from Covance, (Denver, PA). All rabbits were housed in room temperature conditions with a 12 h regular light/dark cycle and ad libitum access to food and water. Each rabbit was submitted to an ophthalmological examination (described below) before and after blast exposure. All experimental work was performed at the U.S. Army Institute of Surgical Research (USAISR) at JBSA Fort Sam Houston in San Antonio, Texas. This study adhered to the tenets of the Association for Research in Vision and Ophthalmology Statement for the Use of Animals in Ophthalmic and Visual Research. This research was conducted in compliance with the Animal Welfare Act by implementing animal welfare regulations and the principles of the National Research Council's Guide for the Care and Use of Laboratory Animals. The facility's Institutional Animal Care and Use Committee (IACUC) approved all research protocols in this study. The facility is fully accredited by the Association for Assessment and Accreditation of Laboratory Animal Care International.

Ophthalmological examinations: Each animal was weighed and anesthetized using an intramuscular injection of ketamine/xylazine (45/5 mg/kg body wt. dose). Prior to the ocular examination, the eyes of the anesthetized rabbits were treated with 1–2 drops of tetracaine hydrochloride, a topical anesthetic ophthalmic solution (Bausch & Lomb, Tampa, FL). Next, 1–2 drops of 1% tropicamide (Bausch & Lomb) were administered for pupil dilation and retinal fundus assessment. Saline was periodically applied to the cornea to

keep the eyes clear and moist during the examination. For ophthalmic evaluations, a dilated slit-lamp exam of both eyes was performed during the baseline examination, immediately after blast wave exposure, and 48 h post-blast. Corneal defects or injuries, such as corneal opacity, abrasions, lacerations, or other injuries to the corneal surface, and retinal hemorrhage were recorded. Changes in CT were determined by corneal confocal scanning laser microscopy (HRT 3, Heidelberg Engineering, Heidelberg, Germany). Vigamox® (Alcon, Fort Worth, TX) and an ophthalmic lubricant (GenTeal®, Alcon) were applied to the eyes at the end of the ophthalmic examinations, at which point the rabbits were placed in a recovery chamber until fully awake and then returned to their cage. Animals with pre-existing ocular pathology were excluded before the start of the study.

Ocular blast injury model: A large, compressed-air-driven shock tube was used in this study to simulate primary blast wave exposure (Figure 1). Detailed descriptions of this system have been provided previously [12]. A rabbit model was adopted because scaling laws suggest that models larger than rat or mouse models are needed to more accurately emulate the blast loading experience in relation to the human eye [12,27]. Prior to blast exposure, the rabbits were anesthetized using ketamine/xylazine as stated above, along with a subcutaneous injection of 2 mg/kg body wt. buprenorphine as an analgesic. Supplemental sedation with isoflurane was used throughout the experiment for maintenance.

Each rabbit from the experimental group was placed in a PVC pipe holder (4-inch inner diameter by 24 inches long) so that the body was protected from the blast wave. The rabbits were then placed in the expansion cone of the shock tube for blast wave exposure. A 0.9% normal saline solution was used to keep the eyes moist throughout the experiment. The rabbits from the experimental group were aligned axially directly in the shock tube so that both eyes would simultaneously receive the same exposure (Figure 1). The rabbits were then exposed to a blast wave peak overpressure of 142.5–164.1 kPa with a positive-phase overpressure impulse (impulse per unit surface area) of 199.6–228.5 Pa-s. The control rabbits were treated identically (including placement in the shock tube) except for the blast exposure.

Immediately after the blast exposure, the rabbits were submitted to an ophthalmic examination, as noted above, to look for any evidence of induced ocular trauma. The rabbits were anesthetized at 48 h post-blast with ketamine and xylazine for follow up of any eye injuries and corneal confocal imaging assessments. The rabbits were then euthanized with an intravenous or intracardiac dose of the veterinary euthanasia solution Fatal-Plus (390 mg/ml phenobarbital, 0.01 mg/ml propylene glycol, 0.29 mg/ml ethyl alcohol, 0.2 mg/ml benzyl alcohol; total dose 150 mg/kg; Vortech Pharmaceuticals, Dearborn, MI), and the eyes were immediately harvested for molecular, biochemical, and immunohistochemical analyses.

In vivo imaging: CT was measured using corneal confocal microscopy images (HRT-Rostock Cornea Module (HRT-RCM), Heidelberg Engineering). An apical z-stack of images was used to estimate CT. A drop of topical anesthetic (tetracaine) was administered in both eyes of anesthetized rabbits. A drop of GenTeal® was placed on the tip of the HRT-RCM objective lens to serve as a thin liquid cushion and to eliminate surface reflections. For CT, scans were made from the epithelial cell layer to the bottom of the endothelial cell layer; images were collected using HRT-RCM streaming software. Five separate volume scans were performed sequentially in the central region of each cornea because the thickness of the cornea exceeded the scanning capabilities of the instrument. Each volume scan consisted of 40 image frames and covered a depth of 77 µm at an acquisition rate of approximately 4.7 frames/s. The starting point for each new scan was set by manually positioning the instrument at the ending position of the previous scan. The field of view for each 384 × 384 pixel image was 400 µm × 400 µm, resulting in a voxel size of 2 µm (z-axis). All image analyses were performed for both eyes of each animal.

RNA isolation, cDNA synthesis, and quantitative PCR (qPCR): Total RNA was isolated from corneal samples (RNeasy® Mini Kit; Qiagen, Germantown, MD) followed by on-column DNase digestion per the manufacturer's instructions. RNA quality and quantity was evaluated using a Nanodrop ND-1000 spectrophotometer (Nanodrop Technologies, Wilmington, DE), and 1 µg total RNA was reverse transcribed (TaqMan, Invitrogen, Carlsbad, CA). The qPCR amplification of AQP1 and AQP5 transcripts and the endogenous control, glyceraldehyde 3-phosphate dehydrogenase (GAPDH), was performed for each template using IQ SYBR® Green Supermix (Bio-Rad, Hercules, CA) and the CFX96 qPCR Detection System (Bio-Rad) using the following protocol: an initial denaturation at 95 °C for 3 min followed by 40 cycles at 95 °C for 10 s and at 60 °C for 30 s. The sequences of primers and probes of AQP1, AQP5, and GAPDH used in this study are listed in Table 1. All experiments were conducted independently at least three times with triplicate reactions for each cDNA tested, and the results were normalized to GAPDH using the ΔΔCt method.

Western blotting: Corneal samples were homogenized in isolation buffer (5% sorbitol, 0.5 mM disodium EDTA, 0.2 mM phenylmethylsulfonyl fluoride, protease inhibitor

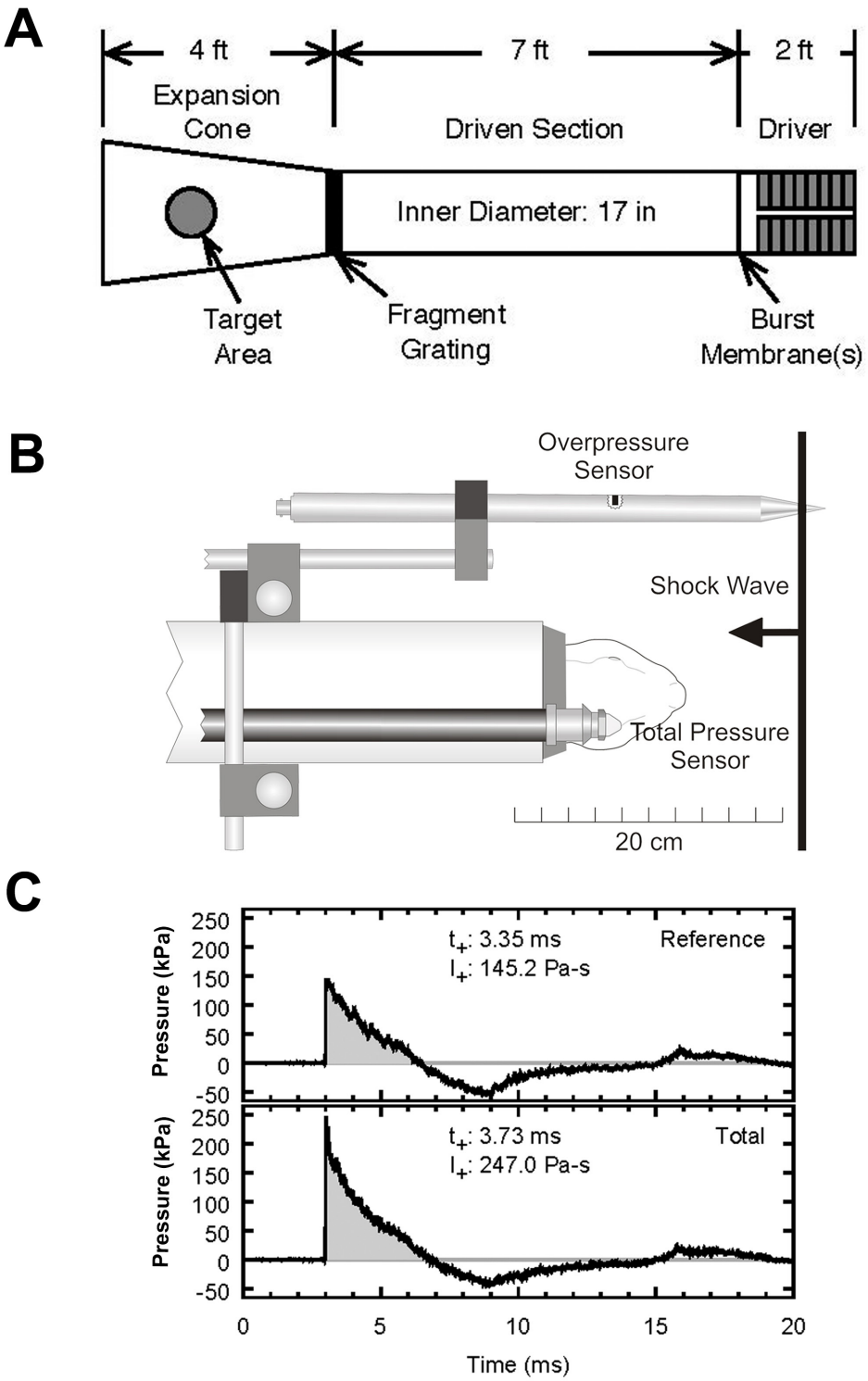

Figure 1. Deployment of a compressed air-driven shock tube to deliver a primary blast effect to rabbit eyes. (**A**) Schematic representation of the air-driven shock tube device. (**B**) Position of pressure sensors relative to target. The bodies of the rabbits are protected by a PVC tube. (**C**) Graph of typical blast overpressure wave profile. Note that the duration of the positive pressure peak is approximately 3 ms.

cocktail, 5 mM histidine-imidazole buffer; pH 7.5) and centrifuged at 2,000 × *g* for 20 min. Proteins (10–20 µg) in the supernatant were denatured in sodium dodecyl sulfate polyacrylamide gel electrophoresis (SDS–PAGE) sample buffer for 20 min at 60 °C, resolved on 4%–20% gradient SDS–PAGE gel (Bio-Rad), and transferred onto nitrocellulose membranes. The membranes were washed with 10 mM Tris-HCl (pH 8.0), 150 mM NaCl, and 0.05% Tween-20 (TBST) and blocked with 5% w/v non-fat dry skim milk in TBST for 1 h at room temperature. Separate membrane blots were probed with AQP1 (1:100 goat polyclonal:SC-9878) and AQP5 (1:100 goat polyclonal:SC-9891) antibodies (Santa Cruz Biotechnology, Santa Cruz, CA) overnight at 4 °C. After rinsing with TBST, all blots were incubated with donkey anti-goat horseradish peroxidase antibody at 1:2000 dilution (Pierce Biotechnology, Inc., Rockford, IL) for 1 h and detected with an enhanced chemiluminescence detection system (Super Signal West Pico Horseradish Peroxidase Detection Kit; Pierce Biotechnology, Inc.). Subsequently, membranes were stripped and probed with anti-β-actin antibody at 1:1000 dilution (SC-47778, Santa Cruz Biotechnology) followed by incubation with 1:2,000 donkey anti-mouse horseradish peroxidase (Pierce Biotechnology, Inc.) as the secondary antibody for normalization. The band intensity was detected using the BioRad ChemiDoc MP imaging system (Bio-Rad). Densitometry analysis of the resulting bands was performed using Image J software (Image J 1.36b; NIH, Rockville Pike, MD).

Immunohistochemistry: Enucleated eyes were fixed for 24 h with modified Davidson's solution (EMS, Hatfield, PA) followed by 10% normal buffered formalin. Fixed samples were dehydrated, embedded in paraffin, and sectioned (4-µm slices) before immunohistochemical labeling. For immunohistochemical labeling, slides were deparaffinized in xylene and rehydrated using a series of 100% ethanol, 95% ethanol, 70% ethanol, and deionized water. Following deparaffinization, an antigen retrieval method was performed using sodium citrate buffer (pH 6) at 85 °C for 15 min. Staining was performed by hydrating the tissue using Hank's balanced salt solution (HBSS). Slides were then blocked using 10% normal horse serum for 30 min, followed by incubation with AQP1 (1:500) and AQP5 (1:50) antibodies for 30 min at room temperature. Following incubation, the antibody was washed with HBSS and probed with a secondary biotinylated horse-anti-goat IgG (1:250, BA-1100, Vector Laboratories, Burlingame, CA) for 1 h, washed with HBSS, and detected with 3,3′-diaminobenzidine (SK-4105, Vector Laboratories). The slides were rinsed in tap water to stop the development of the 3, 3′-diaminobenzidine substrate and then counterstained with Gill's hematoxylin. The slides were dehydrated using the reverse of the deparaffinization treatment described above before putting on coverslips.

Statistical analysis: Data were presented as the mean ± standard error of the mean (SEM) of at least three different experiments, and duplicate or triplicate determinations were performed in each experiment. CT results were subjected to a Wilcoxon sum rank test. For densitometry results of western blot data and relative mRNA abundance data from corneal samples, unpaired *t* tests were performed using SigmaPlot 11.0 (Systat Software, San Jose, CA). A p value <0.05 was deemed to indicate statistical significance.

RESULTS

Slit-lamp examination and corneal thickness measurement: Under slit-lamp examination, corneal abrasions and transient corneal opacities were observed immediately after blast wave exposure of both eyes from three exposed animals but then resolved at 48 h post-blast (Figure 2C-D). No other corneal injuries, such as ocular lacerations, rupture with prolapse, or retinal hemorrhage, were observed with blast wave exposure. No other visible injuries or conditions affecting corneal transparency were observed during baseline examination or at 48 h after blast wave exposure.

Figure 3 shows the CT measurements of experimental and control rabbits obtained via confocal microscopy 48 h post-blast exposure. The mean thickness after blast exposure was 360.0±14.4 µm and 367.0±21.8 µm for right eye corneas (OD) and left eye corneas (OS), respectively. The corneas of the control rabbits had a mean thickness of 294.5±9.8 µm and 300.0±9.6 µm for OD and OS, respectively. The mean thickness of corneas from both eyes before blast exposure at baseline was 303.7±9.2 µm. We observed a significant difference in CT between the blast-exposed rabbits and the control rabbits ($p<0.05$). CT remained elevated up to 18% at 48 h post-blast exposure.

Table 1. Primer used for quantitative PCR.

Gene	Sense primer (5′→3′)	Antisense primer (5′→3′)
GAPDH	GGGTGGTGGACCTCATGGT	CGGTGGTTTGAGGGCTCTTA
AQP1	AGCTGGTGCTGTGTGTGC	AATGCCACAGCCAGTGTAGTC
AQP5	CTGGTGCTGGCATCCTCTA	GCTGGAAGGTGAGGATCAAC

Expression of AQP1 and AQP5 mRNA: Total RNA samples from the corneas of blast-exposed and control rabbits were reverse transcribed and subjected to quantitative PCR to determine the expression of AQP1 and AQP5 using gene-specific primers (Table 1). Transcript levels of AQP1 in whole corneas were 9.3-fold higher in blast-exposed rabbits compared to control rabbits (Figure 4A, $p<0.0001$). Blast-exposed rabbits showed a 1.5-fold increase in AQP5 transcript levels compared to control rabbits, but this was not statistically significant (Figure 4B, $p=0.17$). Quantitative PCR data revealed the upregulation of AQP1 and AQP5 transcripts in the whole cornea after blast exposure.

Protein expression of AQP1 and AQP5: The increase in AQP1 and AQP5 expression at the transcriptional level in rabbit corneas after blast exposure prompted us to determine whether there is a corresponding increase in expression at the protein level. AQP1 and AQP5 protein expression levels in control rabbits and blast-exposed rabbits were analyzed by western blot and normalized to the expression of β-actin, which also served as a loading control. Western blots of whole cornea lysates revealed that both unglycosylated (approx. 29 kDa) and glycosylated (approx. 34 kDa) forms of AQP1 and AQP5 can be detected in control and blast exposed animals (Figure 5A-B). Quantitative densitometry analyses confirmed a blast-induced upregulation of AQP1 and AQP5 expression in the cornea. Figure 5A shows that the total AQP1 level was significantly higher in the blast-exposed rabbits (1.36±0.18) compared to the control rabbits (0.56±0.14; $p<0.05$). AQP5 levels were also significantly higher (Figure 5B) in blast-exposed rabbits (1.23±0.03) compared to control rabbits (0.82±0.07; $p<0.05$).

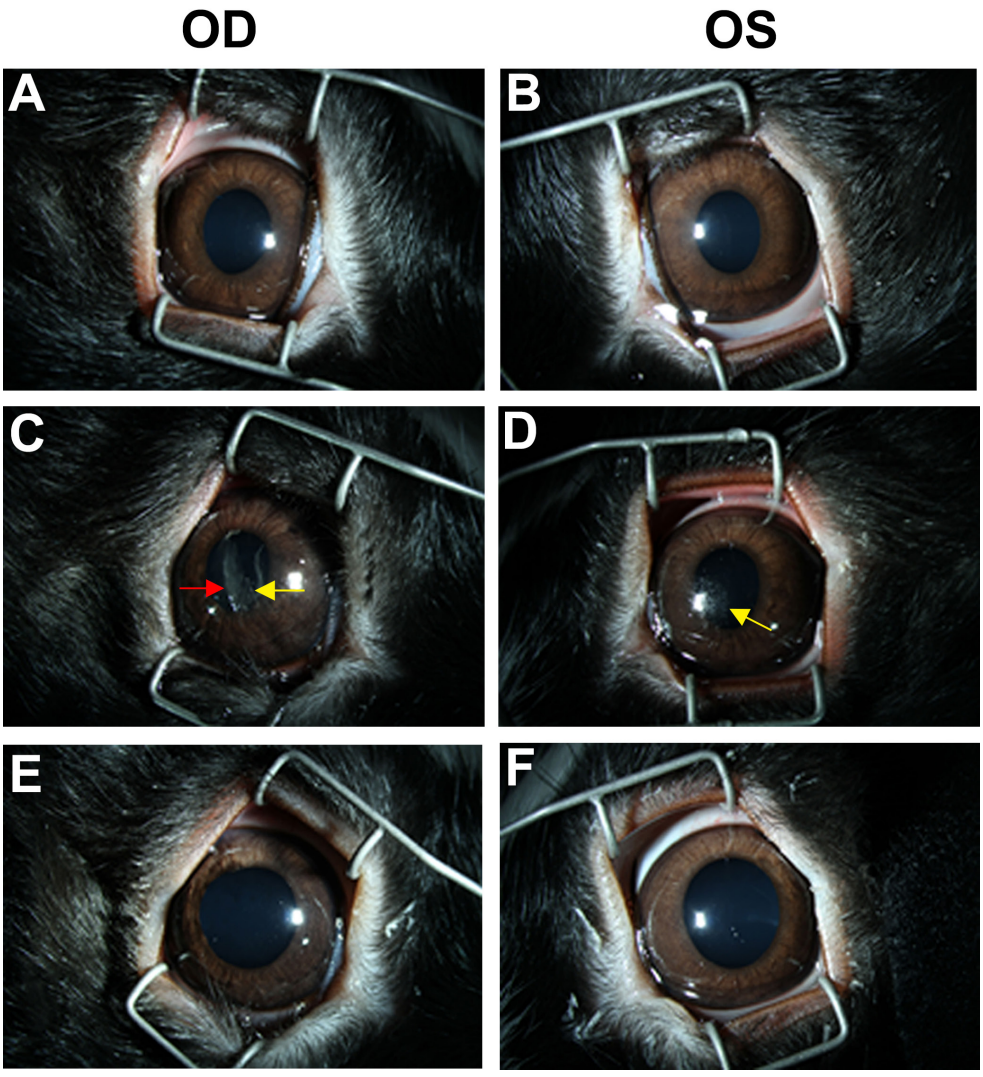

Figure 2. Representative ophthalmic evaluations using a dilated slit-lamp exam of both eyes during baseline (**A–B**), immediately after blast wave exposure (**C–D**), and 48 h post-blast (**E–F**). OD: Right eye; OS: left eye. The red arrow indicates transient corneal opacity, and the yellow arrows indicate corneal abrasion. Data are representative of at least six different animals per group.

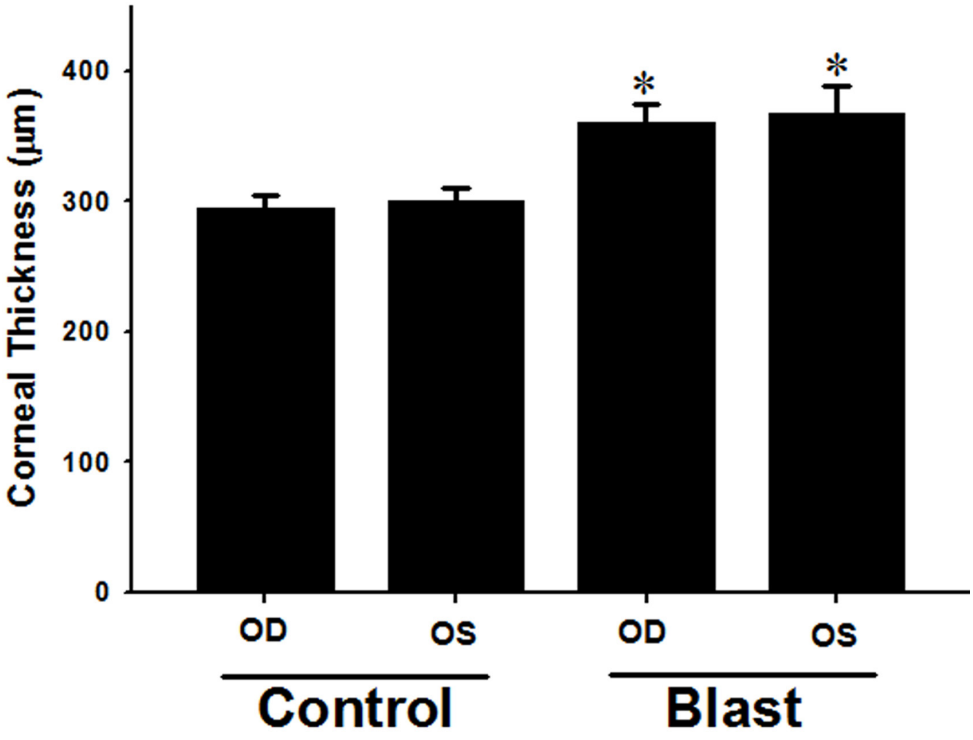

Figure 3. Corneal thickness measurement by confocal microscopy. OD: Right eye; OS: left eye. Scan at 48 h post-blast exposure. *Control cornea compared to blast-exposed cornea ($p<0.05$). Data are presented as mean ± SEM of three to four animals per group.

Immunolocalization of AQP1 and AQP5: Figure 6 shows positive AQP1 and AQP5 staining distributed among different corneal cell layers in both control and blast-exposed rabbit corneas. AQP1 immunostaining (AQP1-IS) was observed in the corneal endothelium and stromal cells in both control and blast-exposed rabbits (Figure 6A-B). Notably, due to blast exposure, IS pattern of AQP1 was altered as evident from AQP1 staining on the membrane of basal side mid-epithelial cells in contrast to the expression on the membrane of superficial corneal epithelial cells (Figure 6B). There was also a focal area of several basal cornea epithelial cells in which the apical, basal, and basolateral aspects of the cell membrane demonstrated strong positive AQP1-IS from blast-exposed rabbits compared to control rabbits (Figure 6B).

In contrast, a mixed AQP5-IS pattern (changed from a mixed membrane and cytoplasmic expression) in the controls

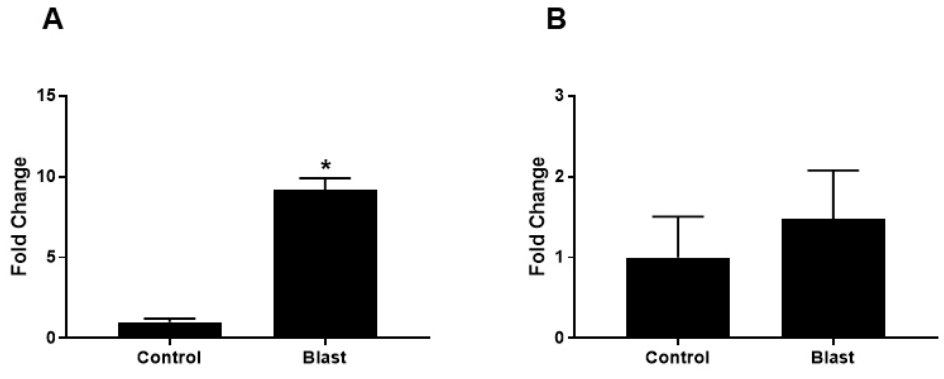

Figure 4. Quantitative PCR (qPCR) of AQP1 and AQP5 transcripts in cornea samples of blast-exposed rabbits. (**A**) The mRNA level for AQP1 was significantly increased ($p<0.0001$) in whole corneas harvested from blast-exposed rabbits compared to those of control rabbits. (**B**) Although the mRNA levels of AQP5 in blast-exposed eyes trended to higher than those in control eyes, the mean difference between the two groups was not statistically significant ($p=0.17$). Data are presented as mean ± SEM of three to five animals per group.

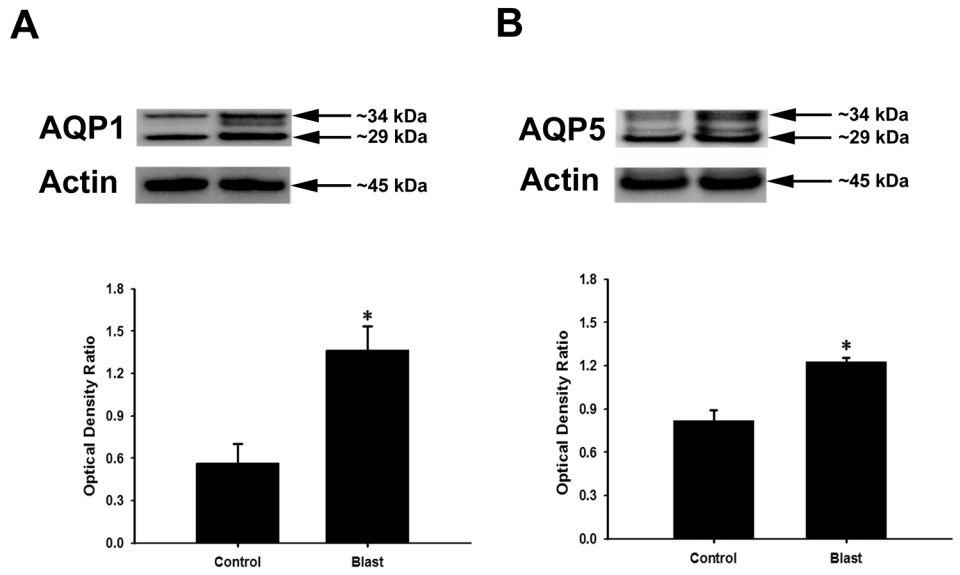

Figure 5. Western blots of AQP1 (**A**) and AQP5 (**B**) proteins isolated from whole cornea homogenates. The densitometry scans of gels are shown in the bottom section of each panel. AQP1 and AQP5 levels were significantly increased in the corneas of blast-exposed rabbits. β-actin was used as the loading control. Arrows indicate molecular weight for AQP1, AQP5, and β-actin. Data are presented as mean ± SEM of six animals per group.

to a predominantly cytoplasmic expression in the basally located epithelial cells in the corneas of blast-exposed rabbits suggests an AQP5 translocation (Figure 6C-D). Minimal AQP5-IS was detected in the corneal stromal keratocytes and corneal endothelial cells of both control and blast-exposed rabbits (Figure 6C-D). Clearly, these images reflect differential expression patterns of AQP1 and AQP5 in the corneas of blast-exposed rabbits compared to those of control rabbits. Altogether, this data indicates that the enhanced expression of AQP1 and changes in the immunolocalization of AQP5 are related to corneal injury arising from elevated blast overpressure.

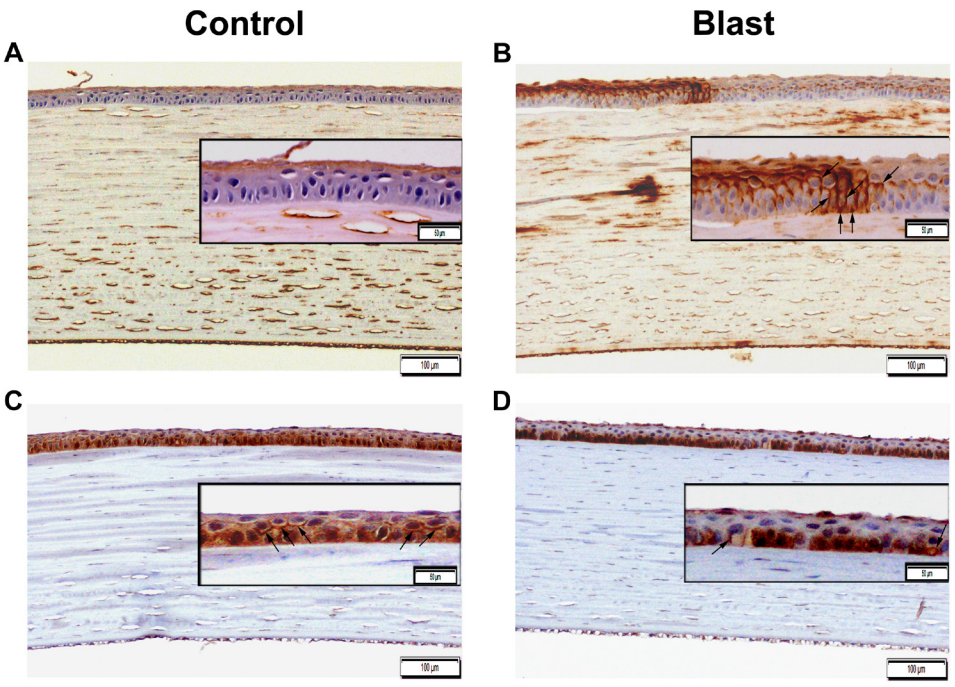

Figure 6. Immunohistochemical localization of AQP1 and AQP5 in the cornea after blast exposure (**B–D**) compared to control (**A–C**). The extent of AQP1 immunostaining increased across the corneal epithelial cells of blast-exposed rabbits (**B**) compared to those of control rabbits (**A**). AQP5 immunostaining changed from a mixed membrane and cytoplasmic expression in the corneal epithelium of control rabbits (**C**) to predominantly cytoplasmic expression in the basally located cornea epithelial cells after blast exposure (**D**). The arrows indicate plasma membrane distribution of the corneal epithelium. The image was captured with 100X (bards=100 µm) and 200X magnification (bards=50 µm).

DISCUSSION

In this study, we have shown that blast exposure induces corneal edema, as evidenced by significant changes in CT and the upregulation of the expression of AQPs. Our results revealed increased CT and are concordant with previous findings correlating a sustained increase in CT with elevated specific impulses that persisted during a 48-h follow-up period [12]. In a report by Jones et al. [12], corneal edema was quantified based on normalized thickness measurements using corneal confocal imaging, which correlated with respective specific impulses, and on histological findings of increased interlamellar voids corresponding to water infiltration [12]. Of note, our study applied a similar approach to demonstrate elevated CT up to 18% in rabbits exposed to blast overpressures of approximately150 kPa. The blast overpressure level used in our injury model was higher than the blast levels used (approximately 117 kPa) by Jones et al. [12].

Slit-lamp examination showed corneal abrasion that resolved 48 h post-blast injury. This finding implies that even in a relatively pristine laboratory environment, blast-propelled particulates can injure the cornea. Changes in CT may play a pivotal role in visual acuity, contrast sensitivity, and perhaps vision-disrupting corneal transparency. The increase in CT persisted at 48 h following blast exposure in our rabbit model, indicating potential similarities with acute or predisposing chronic edema-related diseases, such as PBK and FD, which can cause significant visual impairment. Therefore, it is reasonable to state that CT measurements may emerge as a valuable marker of corneal injury associated with primary blast exposure [13,28]. In addition, corneal transparency requires precise regulation of water and ion content in the corneal epithelium and endothelium. For instance, changes in corneal water content alter the regular diameter and spacing of stromal collagen fibrils that are believed to be critical for corneal transparency [25,29].

In this respect, it is important to note that AQPs take part in transporting water throughout the cornea. AQPs are a family of 13 membrane proteins that function as channels facilitating water transport in response to osmotic gradients. Their localization and function in the eyes and their role in ocular diseases have been extensively reviewed [15,16,22,30]. More importantly, emerging interest in disease-relevant AQPs underscores the great translational potential of AQP-based diagnostics and therapeutics [22,30-32].

Furthermore, the increased expression of AQP1 has been implicated in corneal wound healing [23]. The altered expression of AQPs has been reported in corneal endothelial diseases such as PBK and FD [21]. It is worth mentioning that AQPs are differentially expressed in PBK corneas (decreased AQP1, increased AQP3 and AQP4) and FD corneas (decreased AQP1). Although the presence of both are correlated with vision-disrupting corneal edema, the mechanisms regulating fluid accumulation may differ in individual diseases [21]. Therefore, our observation revealing the altered expression of AQPs, particularly AQP1 and AQP5, in blast-related corneal injury is impactful because these AQPs might emerge as potential therapeutic targets for mitigating blast-induced corneal edema.

Acute and chronic visual problems are frequently experienced by service members and veterans following blast exposure [33,34]. The eye injuries observed in ocular blast injury models are similar to those experienced by service members who have been exposed to IED blasts and blunt trauma [35-38]. For instance, Sherwood et al. reported cornea/iris angle disruptions in a postmortem porcine model following blast wave ranging from 6 psi to 16.6 psi [39]. Moreover, unresolved corneal edema has been observed in a mouse model of blast ocular injury [35]. A possible injury mechanism may involve the high blast wave exerting an energetic torsion to the cornea and thus posterior axial displacement that results in direct contact between the cornea and the lens or iris before the cornea returns to its original position. This blast-mediated injury mechanism may cause corneal epithelial and endothelial cell damage by disrupting the carbonic anhydrase activity and pump-leak mechanism and/or by altering the expression of AQPs associated with water movement. Altogether, these may lead to corneal edema, possibly exacerbating an induced inflammatory response or transiently inducing corneal lymphangiogenesis [13].

In the present study, we found the increased expression of AQPs in corneas after blast wave exposure. We found increased mRNA and protein levels of AQP1 and AQP5 in whole corneas harvested from blast-exposed rabbits compared to those harvested from control rabbits. In blast-exposed corneas, AQP1 mRNA levels were significantly increased (approximately ninefold) compared to matched controls. The mRNA levels of AQP5 in blast-exposed eyes tended to be higher than those in control eyes. A concordant increase in AQP1 immunostaining was also noted in different cornea epithelial cell layers after blast exposure.

With respect to AQP5 subcellular immunolocalization, AQP5 was also localized in the cytosol and cell membranes of epithelial cells from both control and blast-exposed rabbits. However, a predominant cytoplasmic expression in the basally located epithelial cells after blast exposure suggests an alteration in the localization of AQP5 due to either the translocation or internalization of AQP5 following blast exposure.

The plasma membrane expression of AQP5 and its translocation are regulated by multiple pathways [40-42]. In this regard, AQP5 translocation has also been shown to be affected by cAMP in a protein kinase A (PKA)-dependent manner [43]. Intracellular cAMP levels have been shown to regulate AQP5 abundance at the transcriptional level, thus affecting its long-term (≥24 h) sub-cellular distribution [44]. Sidhaye et al. observed a biphasic effect on AQP5 expression and membrane localization when cells expressing AQP5 were exposed to cAMP for short- and long-term periods [43]. For instance, increasing cAMP levels induced a decreased expression of AQP5 in cell membranes in the short term due to increased internalization, followed by an increase in trafficking of AQP5 to the plasma membrane in the long term [43]. This dual response to increased cAMP levels of the trafficking of AQP5 may explain the differences in AQP5 plasma membrane localization in the cornea after primary blast exposure.

It is possible that the immunostaining pattern of AQP5 as seen in the cytosol may be related to the increased trafficking of AQP5 in response to altered cAMP levels after blast exposure. Kumari et al. found that intracellular trafficking and localization of AQP5 expression in corneal epithelial cells are regulated by cAMP through the PKA pathway [45]. They also found that corneas exposed to cAMP (100 µM) for 30 min or 6 h showed a significant decrease in AQP5 from plasma membrane localization, while corneas exposed to the PKA inhibitor H-89 (20 µM) for the same time period had increased AQP5 plasma membrane localization, and the abundance of AQP5 depended upon the extent of exposure [45]. Therefore, it is possible that blast exposure may alter the PKA-mediated regulation of AQP5 in corneal epithelial cells, leading to corneal swelling. AQP5 has recently been shown to participate in other cellular functions, such as cell-to-cell adhesion, cell migration, and cell proliferation [24]. Thus, the increased expression of AQP5 after blast exposure may also be involved in corneal epithelial wound healing by increasing proliferation and potentially stimulating the migration machinery.

Although our blast-injury model showed the increased expression and increased spatial location of AQP1 and AQP5 in blast-exposed corneas at 48 h, further time-course studies are necessary to elucidate the expression of AQP5 in the short term (several hours) and later (72 h to a week) after blast exposure to understand its involvement in injury and the wound-healing response. Further studies are also warranted to identify the underlying mechanisms and signaling pathways of AQP1 and AQP5 vis-à-vis blast exposure.

Given that both AQP1 and AQP5 expression are upregulated, they may contribute to corneal edema resulting from primary blast exposure. Another possibility is that this altered expression is part of the wound-healing process because an increase in the expression of AQPs in contact with the stroma might allow the cells to transport more water into the cornea to enable cell migration and accelerate the healing process [23].

It is tempting to speculate that the significant changes in CT sustained for 48 h and the upregulation of AQPs triggered by blast exposure observed in our injury model could be linked to an inflammatory response to blast exposure. Indeed, Por et al. recently reported that both low-level single and repeated blast exposures can lead to the increased expression of transient receptor potential vanilloid 1 (TRPV1), a polymodal swelling-sensitive cation channel, and the infiltration of neutrophils in corneas in a rat model [46]. Jo et al. found synergistic cooperation between glial AQP4 and TRPV4 in mouse retinas, suggesting potential cross-talk between glial reactivity and edema formation in response to retinal injury [47]. It is plausible that the migration of neutrophils to the site of damage/injury may lead to the amplification of robust inflammatory responses. However, our blast injury rabbit model indicates no infiltration of inflammatory cells to the corneal stroma, despite swelling of the cornea in response to the blast-induced injury. Moreover, the presence of TRVPs was not evaluated in this study. Further studies are necessary to confirm the link between AQP-mediated corneal edema, the expression of TRPV1, and the inflammatory cytokines in our model.

In conclusion, primary blast exposure resulted in edema-related corneal changes characterized by increased CT and the altered expression of AQPs (but not limited to AQP1 and AQP5) with blast overpressure-specific impulses. Nevertheless, we cannot exclude the possibility of the upregulation of other AQP family member(s) not studied here. The findings of this investigation hint at potential acute injury mechanisms indicating that primary blast exposure may increase water permeability. The regulatory role of the elevated expression of AQPs in primary blast-induced ocular injury remains unclear. In-depth studies are warranted to elucidate the underlying mechanisms and the potential role of AQP family members in the detrimental effect of primary blast exposure on corneal tissues.

ACKNOWLEDGMENTS

We are extremely grateful to Andre Akers, Peter Edsall, and William Rowe of the Shock Tube Laboratory, Ocular Trauma Group, US Army Institute of Surgical Research (ISR), Shawn

Chamrad of the ISR Veterinarian Group and MAJ Nathan Wienandt of the ISR Pathology Group for their contributions to animal experiments, as well as to Dr. Jeffrey T. Howard for the statistical analyses. We also thank Dr. Subrata Haldar (ISR) for critical review and editing of the manuscript. The work was supported by the USA Army Medical Research and Material Command under Vision Research Program Grant Number W81XWH-12–2-0055, and the Oak Ridge Institute for Science and Education (ORISE). The opinions or assertions contained herein are the private views of the authors and are not to be construed as official views of the Department of the Army or the Department of Defense.

REFERENCES

1. Abbotts R, Harrison SE, Cooper GL. Primary blast injuries to the eye: a review of the evidence. J R Army Med Corps 2007; 153:119-23. [PMID: 17896542].
2. Scott R. The injured eye. Philos Trans R Soc Lond B Biol Sci 2011; 366:251-60. [PMID: 21149360].
3. Weichel ED, Colyer MH. Combat ocular trauma and systemic injury. Curr Opin Ophthalmol 2008; 19:519-25. [PMID: 18854697].
4. Cockerham GC, Goodrich GL, Weichel ED, Orcutt JC, Rizzo JF, Bower KS, Schuchard RA. Eye and visual function in traumatic brain injury. J Rehabil Res Dev 2009; 46:811-8. [PMID: 20104404].
5. DePalma RG, Burris DG, Champion HR, Hodgson MJ. Blast injuries. N Engl J Med 2005; 352:1335-42. [PMID: 15800229].
6. Wolf SJ, Bebarta VS, Bonnett CJ, Pons PT, Cantrill SV. Blast injuries. Lancet 2009; 374:405-15. [PMID: 19631372].
7. Morley MG, Nguyen JK, Heier JS, Shingleton BJ, Pasternak JF, Bower KS. Blast eye injuries: a review for first responders. Disaster Med Public Health Prep 2010; 4:154-60. [PMID: 20526138].
8. Williams ST, Harding TH, Statz JK, Martin JS. Blast Wave Dynamics at the Cornea as a Function of Eye Protection Form and Fit. Mil Med 2017; 182:S1226-9. [PMID: 28291478].
9. Bricker-Anthony C, Hines-Beard J, Rex TS. Eye-Directed Overpressure Airwave-Induced Trauma Causes Lasting Damage to the Anterior and Posterior Globe: A Model for Testing Cell-Based Therapies. J Ocul Pharmacol Ther 2016; 32:286-95. [PMID: 26982447].
10. Choi JH, Greene WA, Johnson AJ, Chavko M, Cleland JM, McCarron RM, Wang HC. Pathophysiology of blast-induced ocular trauma in rats after repeated exposure to low-level blast overpressure. Clin Experiment Ophthalmol 2015; 43:239-46. [PMID: 25112787].
11. Zou YY, Kan EM, Lu J, Ng KC, Tan MH, Yao L, Ling EA. Primary blast injury-induced lesions in the retina of adult rats. J Neuroinflammation 2013; 10:79-[PMID: 23819902].
12. Jones K, Choi JH, Sponsel WE, Gray W, Groth SL, Glickman RD, Lund BJ, Reilly MA. Low-Level Primary Blast Causes Acute Ocular Trauma in Rabbits. J Neurotrauma 2016; 33:1194-201. [PMID: 26393900].
13. Hos D, Bukowiecki A, Horstmann J, Bock F, Bucher F, Heindl LM, Siebelmann S, Steven P, Dana R, Eming SA, Cursiefen C. Transient Ingrowth of Lymphatic Vessels into the Physiologically Avascular Cornea Regulates Corneal Edema and Transparency. Sci Rep 2017; 7:7227-[PMID: 28775329].
14. Whitcher JP, Srinivasan M, Upadhyay MP. Corneal blindness: a global perspective. Bull World Health Organ 2001; 79:214-21. [PMID: 11285665].
15. Verkman AS, Ruiz-Ederra J, Levin MH. Functions of aquaporins in the eye. Prog Retin Eye Res 2008; 27:420-33. [PMID: 18501660].
16. Schey KL, Wang Z. J LW, Qi Y. Aquaporins in the eye: expression, function, and roles in ocular disease. Biochim Biophys Acta 2014; 1840:1513-23. [PMID: 24184915].
17. Bogner B, Schroedl F, Trost A, Kaser-Eichberger A, Runge C, Strohmaier C, Motloch KA, Bruckner D, Hauser-Kronberger C, Bauer HC, Reitsamer HA. Aquaporin expression and localization in the rabbit eye. Exp Eye Res 2016; 147:20-30. [PMID: 27107794].
18. Hamann S, Zeuthen T, La Cour M, Nagelhus EA, Ottersen OP, Agre P, Nielsen S. Aquaporins in complex tissues: distribution of aquaporins 1–5 in human and rat eye. Am J Physiol 1998; 274:C1332-45. [PMID: 9612221].
19. Macnamara E, Sams GW, Smith K, Ambati J, Singh N, Ambati BK. Aquaporin-1 expression is decreased in human and mouse corneal endothelial dysfunction. Mol Vis 2004; 10:51-6. [PMID: 14758337].
20. Wen Q, Diecke FP, Iserovich P, Kuang K, Sparrow J, Fischbarg J. Immunocytochemical localization of aquaporin-1 in bovine corneal endothelial cells and keratocytes. Exp Biol Med (Maywood) 2001; 226:463-7. [PMID: 11393176].
21. Kenney MC, Atilano SR, Zorapapel N, Holguin B, Gaster RN, Ljubimov AV. Altered expression of aquaporins in bullous keratopathy and Fuchs' dystrophy corneas. J Histochem Cytochem 2004; 52:1341-50. [PMID: 15385580].
22. Verkman AS. Aquaporins in clinical medicine. Annu Rev Med 2012; 63:303-16. [PMID: 22248325].
23. Ruiz-Ederra J, Verkman AS. Aquaporin-1-facilitated keratocyte migration in cell culture and in vivo corneal wound healing models. Exp Eye Res 2009; 89:159-65. [PMID: 19298815].
24. Kumari SS, Varadaraj M, Menon AG, Varadaraj K. Aquaporin 5 promotes corneal wound healing. Exp Eye Res 2018; 172:152-8. [PMID: 29660329].
25. Candia OA, Alvarez LJ. Fluid transport phenomena in ocular epithelia. Prog Retin Eye Res 2008; 27:197-212. [PMID: 18289913].
26. Patil RV, Han Z, Wax MB. Regulation of water channel activity of aquaporin 1 by arginine vasopressin and atrial natriuretic

peptide. Biochem Biophys Res Commun 1997; 238:392-6. [PMID: 9299519].

27. Panzer MB, Wood GW, Bass CR. Scaling in neurotrauma: how do we apply animal experiments to people? Exp Neurol 2014; 261:120-6. [PMID: 25035134].

28. Zhang W, Hu Y, Lu L, Liu Y, Yang X, Sun H, Ruan J, Chen J, Yao Q, Yan C, Gu P, Fu Y, Shao C, Fan X. Rabbit Model of Corneal Endothelial Injury Established Using the Nd: YAG Laser. Cornea 2017; 36:1274-81. [PMID: 28825920].

29. Thiagarajah JR, Verkman AS. Aquaporin deletion in mice reduces corneal water permeability and delays restoration of transparency after swelling. J Biol Chem 2002; 277:19139-44. [PMID: 11891232].

30. Fischbarg J. Water channels and their roles in some ocular tissues. Mol Aspects Med 2012; 33:638-41. [PMID: 22819922].

31. Patil R, Wang H, Sharif NA, Mitra A. Aquaporins: Novel Targets for Age-Related Ocular Disorders. J Ocul Pharmacol Ther 2018; 34:177-87. [PMID: 28632458].

32. Tang G, Yang GY. Aquaporin-4: A Potential Therapeutic Target for Cerebral Edema. Int J Mol Sci 2016; 17:[PMID: 27690011].

33. Capo-Aponte JE, Jurek GM, Walsh DV, Temme LA, Ahroon WA, Riggs DW. Effects of repetitive low-level blast exposure on visual system and ocular structures. J Rehabil Res Dev 2015; 52:273-90. [PMID: 26237153].

34. Goodrich GL, Flyg HM, Kirby JE, Chang CY, Martinsen GL. Mechanisms of TBI and visual consequences in military and veteran populations. Optom Vis Sci 2013; 90:105-12. [PMID: 23314131].

35. Hines-Beard J, Marchetta J, Gordon S, Chaum E, Geisert EE, Rex TS. A mouse model of ocular blast injury that induces closed globe anterior and posterior pole damage. Exp Eye Res 2012; 99:63-70. [PMID: 22504073].

36. Petras JM, Bauman RA, Elsayed NM. Visual system degeneration induced by blast overpressure. Toxicology 1997; 121:41-9. [PMID: 9217314].

37. Rex TS, Reilly MA, Sponsel WE. Elucidating the effects of primary blast on the eye. Clin Experiment Ophthalmol 2015; 43:197-9. [PMID: 25923380].

38. Rossi T, Boccassini B, Esposito L, Iossa M, Ruggiero A, Tamburrelli C, Bonora N. The pathogenesis of retinal damage in blunt eye trauma: finite element modeling. Invest Ophthalmol Vis Sci 2011; 52:3994-4002. [PMID: 21330659].

39. Sherwood D, Sponsel WE, Lund BJ, Gray W, Watson R, Groth SL, Thoe K, Glickman RD, Reilly MA. Anatomical manifestations of primary blast ocular trauma observed in a postmortem porcine model. Invest Ophthalmol Vis Sci 2014; 55:1124-32. [PMID: 24474279].

40. Kitchen P, Oberg F, Sjohamn J, Hedfalk K, Bill RM, Conner AC, Conner MT, Tornroth-Horsefield S. Plasma Membrane Abundance of Human Aquaporin 5 Is Dynamically Regulated by Multiple Pathways. PLoS One 2015; 10:e0143027-[PMID: 26569106].

41. Bragiel AM, Wang D, Pieczonka TD, Shono M, Ishikawa Y. Mechanisms Underlying Activation of alpha(1)-Adrenergic Receptor-Induced Trafficking of AQP5 in Rat Parotid Acinar Cells under Isotonic or Hypotonic Conditions. Int J Mol Sci 2016; 17:[PMID: 27367668].

42. Ishikawa Y, Eguchi T, Skowronski MT, Ishida H. Acetylcholine acts on M3 muscarinic receptors and induces the translocation of aquaporin5 water channel via cytosolic Ca2+ elevation in rat parotid glands. Biochem Biophys Res Commun 1998; 245:835-40. [PMID: 9588201].

43. Sidhaye V, Hoffert JD, King LS. cAMP has distinct acute and chronic effects on aquaporin-5 in lung epithelial cells. J Biol Chem 2005; 280:3590-6. [PMID: 15536076].

44. Yang F, Kawedia JD, Menon AG. Cyclic AMP regulates aquaporin 5 expression at both transcriptional and post-transcriptional levels through a protein kinase A pathway. J Biol Chem 2003; 278:32173-80. [PMID: 12783871].

45. Kumari SS, Varadaraj M, Yerramilli VS, Menon AG, Varadaraj K. Spatial expression of aquaporin 5 in mammalian cornea and lens, and regulation of its localization by phosphokinase A. Mol Vis 2012; 18:957-67. [PMID: 22550388].

46. Por ED, Sandoval ML, Thomas-Benson C, Burke TA, Doyle Brackley A, Jeske NA, Cleland JM, Lund BJ. Repeat low-level blast exposure increases transient receptor potential vanilloid 1 (TRPV1) and endothelin-1 (ET-1) expression in the trigeminal ganglion. PLoS One 2017; 12:e0182102-[PMID: 28797041].

47. Jo AO, Ryskamp DA, Phuong TT, Verkman AS, Yarishkin O, MacAulay N, Krizaj D. TRPV4 and AQP4 Channels Synergistically Regulate Cell Volume and Calcium Homeostasis in Retinal Muller Glia. J Neurosci 2015; 35:13525-37. [PMID: 26424896].

Articles are provided courtesy of Emory University and the Zhongshan Ophthalmic Center, Sun Yat-sen University, P.R. China. The print version of this article was created on 5 June 2019. This reflects all typographical corrections and errata to the article through that date. Details of any changes may be found in the online version of the article.